Journal of Computational Electronics (2020) 19:895–904
https://doi.org/10.1007/s10825-020-01493-7

# DFT and TD-DFT studies of new pentacene-based organic molecules as a donor material for bulk-heterojunction solar cells

**İskender Muz[1] · Mustafa Kurban[2] · Mehmet Dalkilic[3]**

Published online: 13 April 2020


**Abstract**
The performance of organic cells based on bulk heterojunctions (BHJs) has improved recently, but further improvements are necessary. In this work, we have carried out a thorough examination using density functional theory (DFT) and time-dependent (TD)-DFT to investigate the structural and optoelectronic properties of pentacene-based organic molecules (PbOMs) as potential donor material for organic photovoltaic BHJ devices. Our results show that oxadiazole prefers to attach via its nitrogen atoms to the carbon atoms of the pentacene monomer with an adsorption energy about − 32.86 kcal/mol, which means that oxadiazole is efficiently adsorbed on the edge of the pentacene. The HOMO energy level of the PbOM with the lowest bandgap is − 4.00 eV wide, i.e., about 0.86 eV lower and more positive than pentacene, thus providing an ideal open-circuit voltage for photovoltaic devices. The bandgap of the PbOM compounds are about 1.61 and 1.80 eV affording an efficient charge transfer from donor to acceptor. Furthermore, the donor PbOMs are also more stable than the pentacene. We have examined, additionally, the reactivity and absorption properties of individual molecules and PbOM systems. Our results suggest that the PbOM, as a donor material, may significantly improve the efficiency of BHJ solar cells.

**Keywords** Pentacene · Donor material · Bulk-heterojunction · TD-DFT

## 1 Introduction

π-conjugated organic molecules are finding use in such diverse devices as *organic field-effect transistors* (OFETs), organic photovoltaic (OPV) devices, etc. [1–3]., due to their unique properties, e.g., suitable to both the lowest unoccupied molecular orbital (LUMO) and to the highest occupied molecular orbital (HOMO) energy levels, and HOMO–LUMO gaps. Additionally, they possess tunable photophysical properties through designing molecules via the donor–acceptor architecture [4]. More specifically, pentacene—a polycyclic aromatic hydrocarbon—is one of the examples of a π-conjugated organic compound making it a promising candidate for OPV devices [5], because of its high field-effect, electron and hole mobility, and low bandgap properties [6–10]. Pentacene has also been used to form bilayer junctions with $C_{60}$ and perylene [11–16] in efficient organic solar cells and as a hole collector in the dye-sensitized solar cells [17] as well as an electron collector in polymer solar cells [18]. Moreover, pentacene is an electron-donor organic material, so it has been used in OFETs [19] and can be modified for the development of solution processability [20–22]. Moreover, the derivatives of pentacene include desirable properties for organic thin film transistors (OTFTs) and are used as *n*-type organic semiconductors in OTFTs with high electron mobility [23], for solution processing of OFETs due to having a low bandgap, large π-conjugated system, and exhibit good solubility and stability for solution processing of OFETs [24].

A recent study demonstrated that structural modification of pentacene monomers with diacid molecules can be used as a donor for BHJ solar cells [25], thus our motivation for further investigating functionalized pentacene for designing BHJ solar cells.

In this paper, we present our examination of the following structural and optoelectronic properties:

✉ Mustafa Kurban
mkurbanphys@gmail.com

[1] Department of Mathematics and Science Education, Nevşehir Hacı Bektaş Veli University, 50300 Nevşehir, Turkey

[2] Department of Electronics and Automation, Kırşehir Ahi Evran University, 40100 Kırşehir, Turkey

[3] Computer Science Department, Indiana University, Bloomington, IN 47405, USA

- Adsorption energy.
- Ionization potential.
- Electron affinity.
- Chemical hardness.
- HOMO–LUMO gap.
- Refractive index.
- Density of states.
- Charge distributions.
- Electronic charge index and dipole moments.

of pentacene-based organic molecules (PbOMs) as a potential donor material for OPVBHJ devices.

## 2 Computational details

To model the PbOM compounds, individual pentacene and 1,3,4-oxadiazole molecules were optimized and then the position of the 1,3,4-oxadiazole around pentacene based on the structure the lowest total energy was tested. Later, two carbon atoms separately replaced two hydrogen atoms in the meso-point of pentacene as in the TIPS-pentacene molecule, because the substitution of an atom or any molecule on pentacene on the meso-points in a symmetric way also displays higher charge carrier mobility [26, 27]. All the calculations were performed using DFT calculations based on the B3LYP exchange–correlation functional with an empirical dispersion term of Grimme's three-parameter with Becke–Johnson damping (GD3BJ) [28] with 6-311G(*d*,*p*) basis set [29, 30] as implemented in the Gaussian 09 program [31]. The adsorption energy ($E_{ads}$) of all optimized structures was calculated as follows:

$$E_{ads} = E_{compound} - E_{pentacene} - E_{1,3,4\text{ - oxadiazole}} + E_{bsse} \quad (1)$$

where $E_{compound}$ is the total energies of PbOM compound. $E_{pentacene}$ and $E_{1,3,4\text{ - oxadiazole}}$ are the total energy of individual pentacene and 1,3,4-oxadiazole molecules, respectively. $E_{bsse}$ also is defined as the basis set superposition error and calculated using the counterpoise correction method [32]. The adiabatic ionization potential (AIP) and vertical ionization potential (VIP) of all optimized structures were calculated as follows:

$$\text{AIP/VIP} = E_{cation} - E_{neutral} \quad (2)$$

where the AIP is the energy difference between the ground state of the cation $\left(E_{cation}\right)$ and the ground state of the neutral $\left(E_{neutral}\right)$. VIP is defined as the energy difference between the $E_{cation}$ and $E_{neutral}$ of the neutral optimized geometry. To elucidate the stability and chemical reactivity of the PbOM compounds, the quantum chemical descriptors, including chemical hardness ($\eta$), chemical potential ($\mu$), electrophilicity index ($\omega$), and maximum amount of electronic charge index $\left(\Delta N_{max}\right)$, were calculated as follows [33, 34]

$$\left[\eta = (\text{IP} - \text{EA})/2\right],\ \left[\mu = -(\text{IP} + \text{EA})/2\right],\ \left[\omega = \mu^2/2\eta\right] \text{ and } \left[\Delta N_{max} = -\mu/\eta\right] \quad (3)$$

where IP and EA correspond to ionization potential and electron affinity, respectively. According to Koopman's theorem, the energies of the HOMO and LUMO orbitals are given by IP $\approx -E_{HOMO}$ and EA $\approx -E_{LUMO}$. The natural bond orbital calculations were performed to understand both the charge distributions and the nature of donor–acceptor interactions. GaussSum program [35] is implemented to plot density of states (DOS). Time-dependent (TD)-DFT calculation based on CAM-B3LYP functional [36] with 6-311G(*d*,*p*) basis set was performed for estimating absorption spectra, because B3LYP underestimates exited state energies when compared CAM-B3LYP [37, 38] and LC-BLYP functionals [39–42]. Moreover, B3LYP has a 0.2 fraction of exchange, and thus it does not possess the correct asymptotic form of the exchange–correlation potential while CAM-B3LYP and LC-BLYP functionals have 0.65 and 1.0 fraction of exchange, respectively.

The open-circuit voltage ($V_{OC}$) of organic photovoltaic BHJ devices can be analyzed by [43]

$$V_{OC} = \frac{1}{e}\left(\left|E^{D}_{HOMO}\right| - \left|E^{A}_{LUMO}\right|\right) - 0.3\,\text{V} \quad (4)$$

We presumed an energy difference $\Delta E$ of 0.3 eV between the HOMO of the donor $\left(E^{D}_{HOMO}\right)$ and the LUMO of the acceptor $\left(E^{A}_{LUMO}\right)$ representing the energy loss.

## 3 Results and discussions

### 3.1 Structure, energy, and stability

We began by studying the behavior of 1,3,4-oxadiazole molecule around the pentacene without making structural modifications. The optimized structures of the oxadiazole molecule(s) adsorbed pentacene. In Fig. 1, we illustrate bond distances and the energy gaps of HOMO and LUMO for B3LYP/6-311G(*d*,*p*). In Fig. 2, we show the geometries and point groups (P.G.) of modified pentacene compounds and the oxadiazole molecule, which are fully optimized. Different initial configurations including O, N and H atoms of oxadiazole molecule approach to C atom, and at the edge of the PbOM is encouraged to provide the most suitable adsorption structure. As shown in Fig. 2b, c, oxadiazole molecules

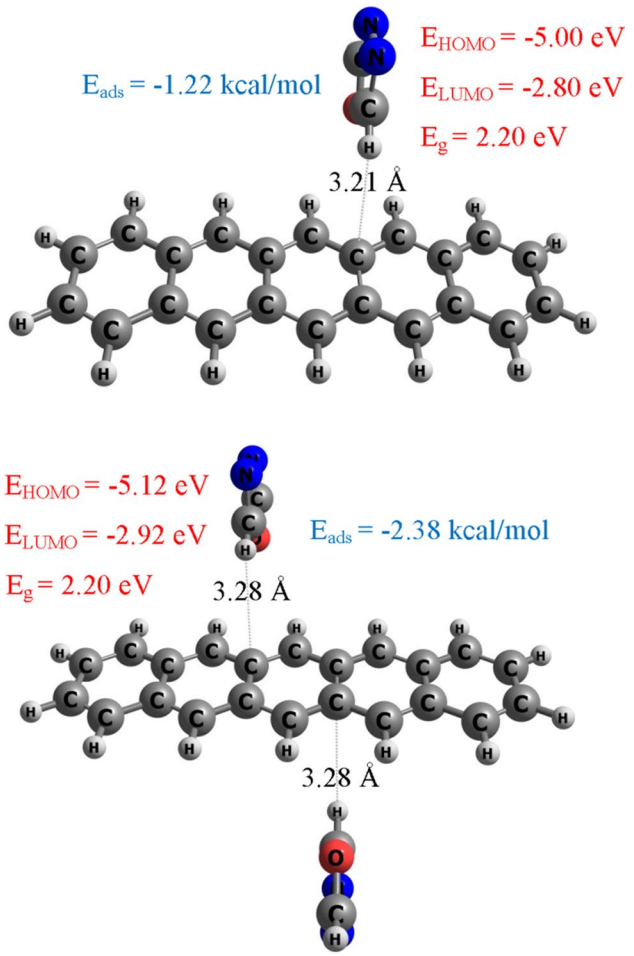


**Fig. 1** The optimized structures of 1,3,4-oxadiazole molecule(s) adsorbed pentacene, as well as the adsorption energies and the energy gaps of HOMO and LUMO at B3LYP/6-311G(*d*,*p*) level of theory (Colour online)

prefer to connect via its N atoms to C atoms at the edge of the PbOM. Adsorption energies ($E_{ads}$) calculated using dispersion corrected DFT-B3LYP method is listed in Table 1. $E_{ads}$ values of PbOM-1 and PbOM-2 compounds are negative and lie at − 22.20 and − 32.86 kcal/mol, respectively. These results demonstrate that the interactions of PbOM with oxadiazole are suitable processes. In addition, the PbOM-2 compound has greater negative adsorption energy than the PbOM-1, and so, it is more stable. It is important to note that PbOM-2 compound may be used as a potential electron transport material.

The optimized structure of pentacene has the C–C bond length 1.43 Å and the C–C–C and C–C–Hangles are 120.6° and 119.2°, respectively. Moreover, the optimized structure of PbOM has the C–C bond length 1.40 Å and the C–C–C and C–C–Hangles are 120.3° and 119.5°, respectively. The C–H bond length is found to be 1.08 Å which remained unchanged for pentacene and all the PbOM compounds. Moreover, the calculated structural parameters for pentacene are in agreement with experimental values [44] and previous studies [45, 46]. On the other hand, interaction bond lengths between C atom at the edge of the PbOM and N atom of oxadiazole molecule (s) are found to be 1.315 Å and 1.309 Å for PbOM-1 and PbOM-2, respectively. Therefore, the interaction bond lengths are consistent with the more negative adsorption energy in PbOM-2 which is the more stable compound.

### 3.2 HOMO–LUMO energy gap, density of states and charge transfer

Figure 3 shows the HOMO and LUMO energy gaps ($E_g$) which are fully optimized for B3LYP, TPSS and ωB97XD methods with the 6-311G(*d*,*p*) basis set. The HOMO and LUMO energy levels in the pentacene are − 6.97 and − 4.30 eV, respectively, indicating a low conductivity. In addition, the HOMO and LUMO energy levels in the oxadiazole molecule are − 8.08 and − 0.77 eV, respectively. These results indicate that pentacene is kinetically and thermally stable, whereas the oxadiazole is more reactive. After the oxadiazole adsorption process on PbOM, the HOMO levels sharply increased, while the LUMO levels in PbOM-1 and PbOM-2 compounds only slightly increased (see Fig. 4 and Table 1), and so $E_g$ is changed. Besides, the calculated $E_g$ value (2.20 eV) for the pentacene for B3LYP/6-311G(*d*,*p*) agrees with the experimental [47] value of 2.15 eV. In this study, $E_g$ value for the PbOM is found to be 2.49 eV. $E_g$ is decreased from 2.49 to 1.80 eV (for PbOM-1) and 1.62 eV (for PbOM-2) when PbOM adsorbed the oxadiazole molecule(s). Thus, on the one hand, PbOM-1 and PbOM-2 possess ideal band with low bandgap for OPV. On the other hand, the HOMO energy level of oxadiazole is larger than that of PbOM, indicating that oxadiazole is the electron donor. The LUMO of oxadiazole is smaller than that of PbOM indicating that it is an acceptor. $E_g$ is a critical parameter in determining charge transfer phenomenon, chemical reaction, and electronic conductivity. We see, then, that PbOM-1 and PbOM-2 compounds exhibit higher chemical reactivity than PbOM or pentacene. Similarly, there is a significant increase in conductivity of PbOM-1 and PbOM-2 compounds compared to either pentacene or PbOM; we establish this order is as follows: PbOM < Pentacene < PbOM-1 < PbOM-2. From our results, we can conclude that the PbOM-2 compound is the more

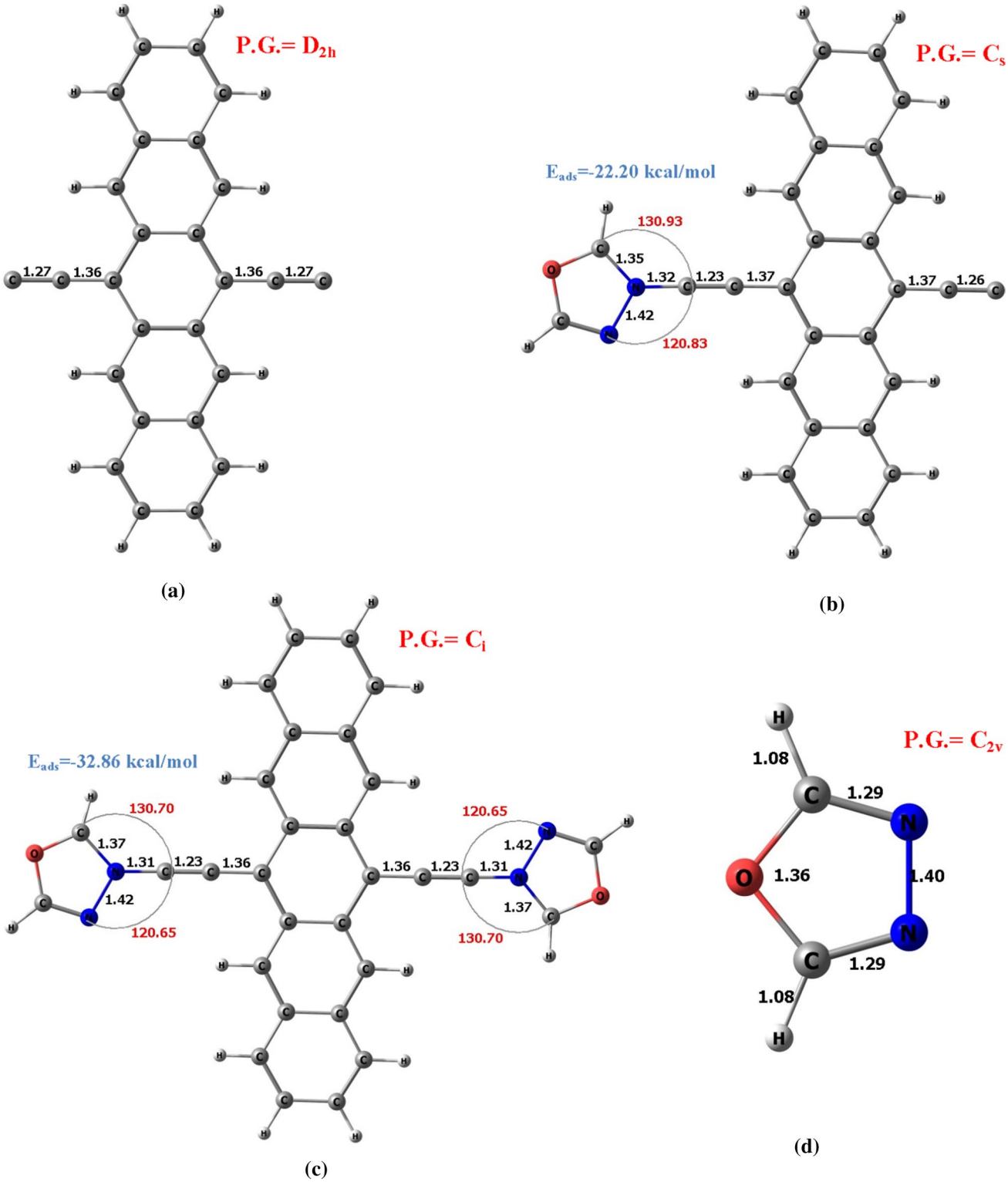


**Fig. 2** The optimized structures of **a** PbOM, **b** PbOM-1, **c** PbOM-2 compounds and **d** 1,3,4-oxadiazole molecule at B3LYP/6-311G(*d*,*p*) level of theory (Colour online)

**Table 1** The electronic and reactivity properties of the oxadiazole, pentacene, PbOM, PbOM-1 and PbOM-2 compounds

| | Oxadiazole | Pentacene | PbOM | PbOM-1 | PbOM-2 |
|---|---|---|---|---|---|
| $E_{ads}$ | – | – | – | −4.05 | −4.72 |
| AIP | 10.63 | 6.13 | 11.01 | 9.22 | 8.35 |
| VIP | 11.31 | 6.18 | 11.14 | 9.28 | 8.54 |
| HOMO | −8.08 | −4.86 | −6.79 | −4.91 | −4.00 |
| LUMO | −0.77 | −2.66 | −4.30 | −3.11 | −2.38 |
| $E_g$ | 7.31 | 2.20 | 2.49 | 1.80 | 1.61 |
| $eV_{oc}$ | – | 1.33 | 3.26 | 1.21 | 0.47 |
| $\eta$ | 3.65 | 1.10 | 1.24 | 0.90 | 0.81 |
| $\mu$ | −4.42 | −3.76 | −5.54 | −4.01 | −3.19 |
| $\omega$ | 2.68 | 6.41 | 12.35 | 8.94 | 6.31 |
| $\Delta N_{tot}$ | 1.21 | 3.41 | 4.46 | 4.46 | 3.96 |
| $\mu_D$ | 3.14 | 0.00 | 0.00 | 16.41 | 0.01 |

Values are in eV except dipole moment (Debye). $V_{oc}$ values are calculated using the LUMO of $C_{60}$ as an acceptor

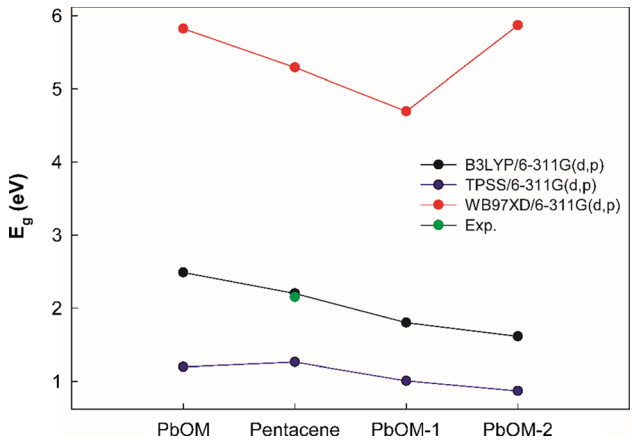


**Fig. 3** The HOMO–LUMO energy gaps $(E_g)$ calculated using different methods for pentacene, PbOM, PbOM-1 and PbOM-2 compounds (Colour online)

suitable candidate as a donor material for organic electronics, because the small band gap easily makes promotion of electrons in photovoltaics. We have mentioned about $V_{OC}$ of the organic solar cells depends on the energy gap between $E^D_{HOMO}$ and $E^A_{LUMO}$ in Sect. 2. Our results show that $C_{60}$, as an acceptor material, the $V_{OC}$ values range from 3.26 to 0.47 eV. The $V_{OC}$ (0.47 eV) is lower than the bandgap of PbOM-2 (1.61 eV), while it (3.26 eV) is greater than bandgap of PbOM (2.49 eV). Thus, the narrow bandgap of PbOM-2 with low-lying HOMO energy level is the desired energy band alignment to use as photovoltaic material.

To obtain detailed information on electronic states in the pentacene, PbOM, PbOM-1 and PbOM-2 compounds, we report in this study the results of the electronic total DOS as seen in Fig. 5. The density of localized states decreases concomitantly along with oxadiazole molecule where the greatest contribution comes from the PbOM molecule. These fluctuations progressively disappear based on the substitution of the oxadiazole molecule to the pentacene. The density of localized states has a sharply increasing tendency to occur in the region of between − 10 and − 15 eV. In addition, the DOS plots show a sign anomaly change in the gap regions. The molecular electrostatic potential (MEP) maps are also presented in Fig. 5, and the plots of MEP are from 0.02 to 0.02 au. The DOS and MEP of these compounds provides some information on the electronic structure. The MEP maps show that the negative charge is mainly concentrated at the nitrogen and oxygen.

AIP and VIP values are associated with an effect of electron donating as two significant characteristics of the electronic structure. As given in Table 1, the calculated AIP and VIP values (6.13 eV and 6.18 eV) for pentacene for B3LYP/6-311G(*d*,*p*) again agrees with the experimental [48] value of 6.58 eV. The AIP and VIP values for the PbOM are 11.01 and 11.14 eV, respectively. AIP is decreased from 11.01 to 9.22 eV (for PbOM-1) and 8.35 eV (for PbOM-2) when PbOM adsorbed oxadiazole molecule(s). Similarly, VIP is decreased from 11.14 to 9.28 eV (for PbOM-1) and 8.54 eV (for PbOM-2). Results demonstrate that PbOM is the most available structure to accepting electrons. Note that VIP values are higher than AIP values due to energy compensation.

Atomic charges affect dipole moment, electronic, and molecular properties, giving a clear indication of the charge transfer [49]. We have also investigated the charge distributions of the PbOM, PbOM-1 and PbOM-2 compounds including Mulliken and natural population analyses (NPA). Charge distribution calculations are a useful way to explain the differences in electropositivity and electronegativity of atoms within the compound. Figure 6a, b shows Mulliken and NPA charge distributions of PbOM, PbOM-1 and PbOM-2 compounds. Charges of carbon, hydrogen, nitrogen and oxygen atoms are presented in red, green, blue and cyan colors, respectively (see Fig. 6). Atomic charges in the PbOM are transferred from hydrogen to carbon. According to Mulliken and NPA analyses, both the nitrogen (−0.37/−0.14 |*e*|) and oxygen atoms (−0.43/−0.19 |*e*|) of PbOM-1 compound carried a notable negative charges, and both carbon 0.20/0.38 |*e*| and hydrogen atoms (0.15/0.18 |*e*|) showed positive. A similar trend is observed for PbOM-2 compound. The nitrogen (−0.33/−0.17 |*e*|) and oxygen

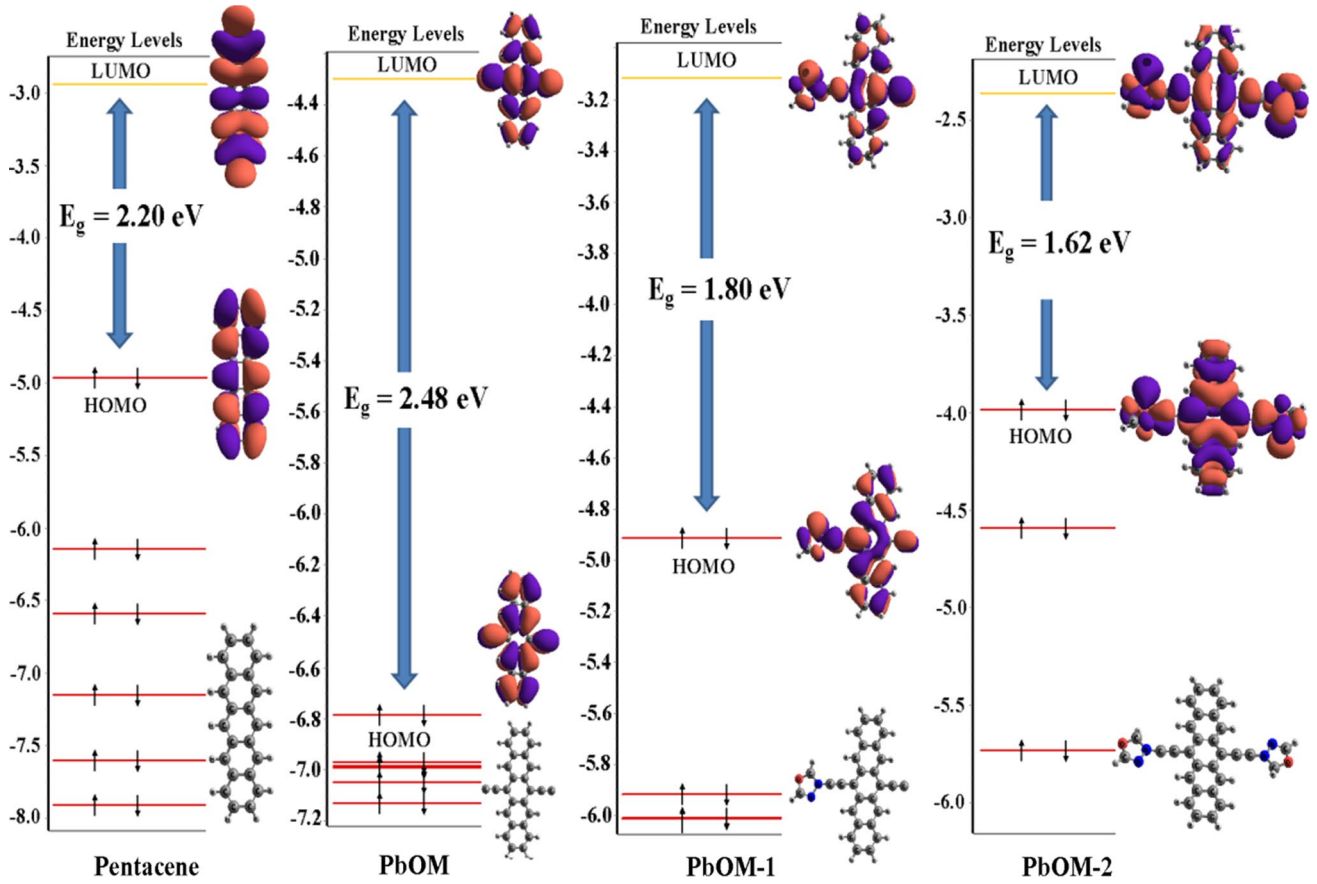


**Fig. 4** The HOMO and LUMO energy levels of the pentacene, PbOM, PbOM-1 and PbOM-2 compounds at B3LYP/6-311G(*d*,*p*) level of theory (Colour online)

atoms (−0.45/−0.20 |*e*|) of PbOM-2 compound carried a high negative charge; however, carbon 0.20/0.38 |*e*| and hydrogen atoms (0.15/0.18 |*e*|) had a positive charge suggesting their electron accepting behavior. It is important that there is a significant change in charge transfer due to adsorbed oxadiazole molecule(s). PbOM, inside PbOM-1 and PbOM-2compounds, becomes an acceptor ($A^+$), whereas oxadiazole molecule behaves like adonor ($D^-$) (see Fig. 6). Note that the Mulliken analysis is found to be compatible with NPA.

### 3.3 Global reactivity descriptors

We examined the reactivity properties of PbOM compounds, i.e., chemical hardness ($\eta$), chemical potential ($\mu$), electrophilicity index ($\omega$), and the maximum amount of electronic charge index ($\Delta N_{tot}$). The values of $\eta$, $\mu$, $\omega$ and $\Delta N_{tot}$ are presented in Table 1. As PbOM adsorbed oxadiazole molecule(s), $\eta$, $\mu$, $\omega$ and $\Delta N_{tot}$ are decreased significantly from 1.24 eV to 0.81, from 12.35 eV to 6.31 and 4.46 eV to 3.96, respectively. Parr et al. reported that the stable compounds must have lower electrophilicity index [50]. It is important to note that there is an increase in stability of PbOM-1 and PbOM-2 compounds compared to the PbOM. This order is as follows: PbOM < PbOM-1 < PbOM-2. The propensity of electron acceptors of the compound is decreased when pentacene adsorbed oxadiazole molecule(s). In addition, $\mu$ is increased for PbOM-1 and PbOM-2 compounds. PbOM-1 and PbOM-2 compounds show a good electrophile characteristic due to a high value of $\mu$ and a low value of $\eta$.

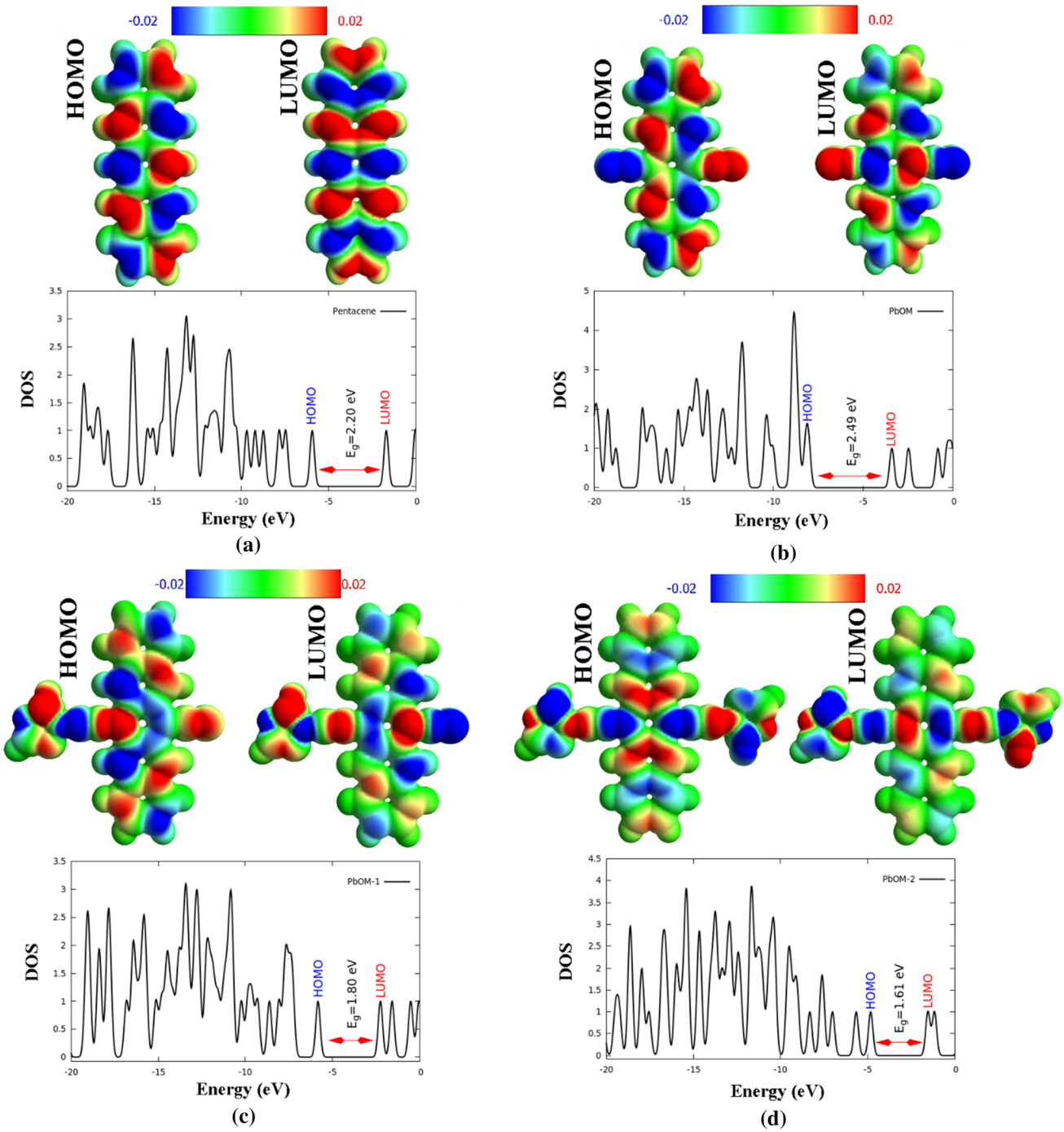


**Fig. 5** The DOS and MEPs of the **a** pentacene, **b** PbOM, **c** PbOM-1 and **d** PbOM-2 compounds at B3LYP/6-311G(*d*,*p*) level of theory (Colour online)

### 3.4 Refractive index and absorption spectra

We have investigated the optical properties of PbOM compounds: refractive index and absorption spectra. Hervé and Vandamme [51] found a relationship between the HOMO–LUMO gap $\left(E_g\right)$ and refractive index $(n)$ in semiconductors as formalized as:

$$n^2 - 1 = A^2/\left(E_g + B\right)^2 \tag{5}$$

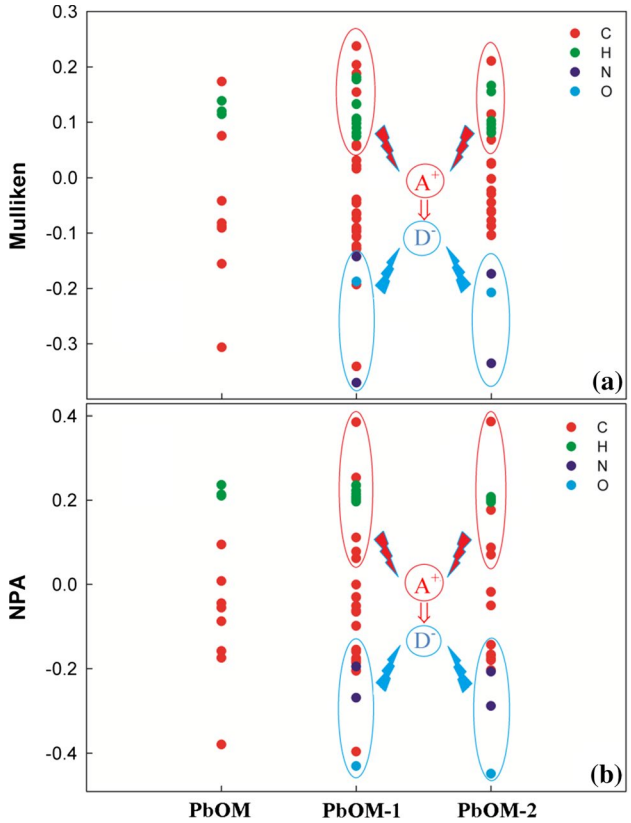


**Fig. 6** Charge distributions **a** the Mulliken and **b** NPA of PbOM compounds at B3LYP/6-311G(*d*,*p*) level of theory (Colour online)

**Table 2** The refractive indexes of the oxadiazole, pentacene, PbOM, PbOM-1 and PbOM-2 compounds

| | Oxadiazole | Pentacene | PbOM | POD-1 | POD-2 |
|---|---|---|---|---|---|
| Hervé–Vandamme | 1.61 | 2.60 | 2.49 | 2.77 | 2.86 |
| Kumar-Singh | 1.77 | 2.61 | 2.51 | 2.79 | 2.89 |
| Moss relation | 1.90 | 2.56 | 2.49 | 2.70 | 2.77 |
| Reddy | 2.17 | 3.03 | 2.92 | 3.22 | 3.33 |
| Exp. | 1.42 | 1.81 | – | – | – |

Here, $A$ (13.6 eV) and $B$ (3.4 eV) are a constant. The $n$ of the PbOM, PbOM-1 and PbOM-2 compounds are calculated from Eq. 5, and the results are given in Table 2.

The calculated $n$ values of oxadiazole (1.61) and pentacene (2.60) using Eq. 1. Agree with the experimental values of 1.42 and 1.81, respectively. Note that these values are the closest to the experimental values among various relationships, for example, in Moss, Reddy, Kumar-Singh [51]. In addition, $n$ values are increased from 2.49 to 2.77 (for PbOM-1) and 2.86 (for PbOM-2). We note that $n$ values increase inversely based on a decrease in the energy band gaps from Eq. 1. This result indicates that there is a general trend in an increase in refractive index as PbOM absorbed oxadiazole molecule(s). Thus, PbOM-1 and PbOM-2 possess ideal band with low bandgap and broad and strong absorption in visible and NIR region.

Figure 7 displays the absorption spectra of PbOM compounds. It was observed that there is an increasing trend in absorbance values in the range of 546–566 nm. We can conclude that the PbOM-1 and PbOM-2 compounds give rise to an enhancement in absorption spectra in the visible region. Especially, the PbOM-1 and PbOM-2 need the lowest energy (2.190 eV) in the absorbance maxima.

## 4 Conclusions

We carried out a theoretical study to model PbOM compounds as a donor material for organic photovoltaic bulk-heterojunction devices. In our work, the structural and optoelectronic properties such as adsorption energy, ionization potential, electron affinity, chemical hardness, HOMO–LUMO gap, refractive index, density of states, charge distributions, electronic charge index, dipole moments and absorption spectra of the PbOM compounds were investigated by DFT and TD-DFT calculations for first time. Compared to the pentacene molecule, the PbOM compounds have more desirable properties. For instance, the PbOM-2 compound is more stable due to its greater negative adsorption energy. The band gaps of the PbOM compounds are found to be smaller than those of the individual pentacene and oxadiazole molecules. The HOMO energy level of the PbOM-2 compound is more positive than the pentacene, so it reduces the open-circuit voltage of the solar cell. The band gap of the PbOM-1 and PbOM-2 compounds are about 1.61 and 1.80 eV which provide efficiently charge transfer from donor to acceptor. The refractive indices of the PbOM compounds are greater than pentacene. The PbOM-1 has the largest dipole moment which means that it has the strongest

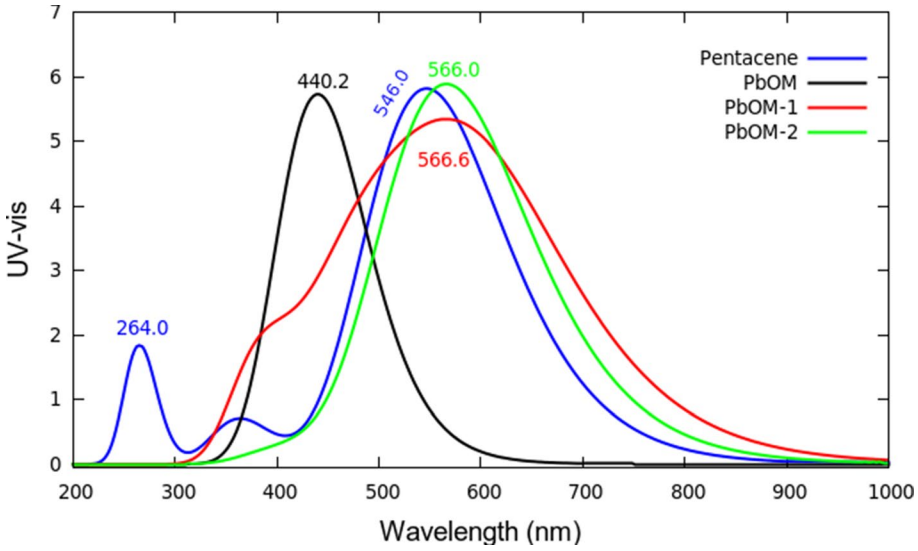


**Fig. 7** The UV–vis spectra of the pentacene and PbOM compounds at CAM-B3LYP/6-311G(*d*,*p*) level of theory (Colour online)

intermolecular interaction. The charge distributions of pentacene are considerably changed along with the oxadiazole molecule. The PbOM-1 and PbOM-2 compounds give rise to an enhancement in absorption spectra in the visible region. We hope that the obtained results will provide an insight to experimental studies to design new kinds of photovoltaic devices with higher efficiency.

**Acknowledgments** The numerical calculations reported were partially performed at TUBITAK ULAKBIM, High Performance and Grid Computing Centre (TRUBA resources), Turkey.

## References

1. Duan, C., Zhang, K., Zhong, C., Huang, F., Cao, Y.: Recent advances in water/alcohol-soluble π-conjugated materials: new materials and growing applications in solar cells. Chem. Soc. Rev. **42**, 9071–9104 (2013)
2. Beaujuge, P.M., Fréchet, J.M.J.: Molecular design and ordering effects in π-functional materials for transistor and solar cell applications. J. Am. Chem. Soc. **133**, 20009–20029 (2011)
3. Facchetti, A.: π-conjugated polymers for organic electronics and photovoltaic cell applications. Chem. Mater. **23**, 733–758 (2011)
4. Kitamura, T., Ikeda, M., Shigaki, K., Inoue, T., Anderson, N.A., Ai, X., Lian, T., Yanagida, S.: Phenyl-conjugated oligoene sensitizers for $TiO_2$ solar cells. Chem. Mater. **16**, 1806–1812 (2004)
5. Lin, Y.Y., Gundlach, D.J., Nelson, S.F., Jackson, T.N.: Pentacene-based organic thin-film transistors. IEEE Trans. Electron Devices **44**, 1325–1331 (1997)
6. Nelson, S.F., Lin, Y.Y., Gundlach, D.J., Jackson, T.N.: Temperature-independent transport in high-mobility pentacene transistors. Appl. Phys. Lett. **72**, 1854–1856 (1998)
7. Dimitrakopoulos, C.D., Malenfant, P.R.L.: Organic thin film transistors for large area electronics. Adv. Mater. **14**, 99–117 (2002)
8. Chason, M., Brazis, P.W., Zhang, H., Kalyanasundaram, K., Gamota, D.R.: Printed organic semiconducting devices. Proc. IEEE **93**, 1348–1356 (2005)
9. Yang, H., Shin, T.J., Ling, M.-M., Cho, K., Ryu, C.Y., Bao, Z.: Conducting AFM and 2D GIXD studies on pentacene thin films. J. Am. Chem. Soc. **127**, 11542–11543 (2005)
10. Heringdorf, F., Reuter, M.C., Tromp, R.M.: Growth dynamics of pentacene thin films. Nature **412**, 517–520 (2001)
11. Yang, J., Nguyen, T.-Q.: Effects of thin film processing on pentacene/C60 bilayer solar cell performance. Org. Electron. **8**, 566–574 (2007)
12. Nanditha, D.M., Dissanayake, M., Hatton, R.A., Curry, R.J., Silva, S.R.P.: Operation of a reversed pentacene-fullerene discrete heterojunction photovoltaic device. Appl. Phys. Lett. **90**, 113505 (2007)
13. Pandey, A.K., Unni, K.N.N., Nunzi, J.-M.: Pentacene/perylene co-deposited solar cells. Thin Solid Films **511–512**, 529–532 (2006)
14. Yoo, S., Domercq, B., Kippelen, B.: Efficient thin-film organic solar cells based on pentacene/C60 heterojunctions. Appl. Phys. Lett. **85**, 5427–5429 (2004)
15. Yoo, S., Domercq, B., Kippelen, B.: Intensity-dependent equivalent circuit parameters of organic solar cells based on pentacene and C60. J. Appl. Phys. **97**, 103706 (2005)
16. Pandey, A.K., Nunzi, J.-M.: Efficient flexible and thermally stable pentacene/C60 small molecule based organic solar cells. Appl. Phys. Lett. **89**, 213506 (2006)
17. Senadeera, G.K.R., Jayaweera, P.V.V., Perera, V.P.S., Tennakone, K.: Solid-state dye-sensitized photocell based on pentacene as a hole collector. Sol. Energy Mater. Sol. Cells **73**, 103–108 (2002)
18. Unni, K.N.N., Pandey, A.K., Alem, S., Nunzi, J.-M.: Ambipolar organic field-effect transistor fabricated by co-evaporation of pentacene and *N*,*N*′-ditridecylperylene-3,4,9,10-tetracarboxylic diimide. Chem. Phys. Lett. **421**, 554–557 (2006)
19. Anthony, J.E.: The larger acenes: versatile organic semiconductors. Angew. Chem. Int. Ed. **47**, 452–483 (2008)
20. Lloyd, M.T., Mayer, A.C., Tayi, A.S., Bowen, A.M., Kasen, T.G., Herman, D.J., Mourey, D.A., Anthony, J.E., Malliaras, G.G.: Photovoltaic cells from a soluble pentacene derivative. Org. Electron. **7**, 243–248 (2006)
21. Lloyd, M.T., Mayer, A.C., Subramanian, S., Mourey, D.A., Herman, D.J., Bapat, A.V., Anthony, J.E., Malliaras, G.G.: Efficient solution-processed photovoltaic cells based on an anthradithiophene/fullerene blend. J. Am. Chem. Soc. **129**, 9144–9149 (2007)
22. Palilis, L.C., Lane, P.A., Kushto, G.P., Purushothaman, B., Anthony, J.E., Kafafi, Z.H.: Organic photovoltaic cells with high

open circuit voltages based on pentacene derivatives. Org. Electron. **9**, 747–752 (2008)
23. Tang, Q., Liang, Z., Liu, J., Xu, J., Miao, Q.: *N*-Heteroquinones: quadruple weak hydrogen bonds and n-channel transistors. Chem. Commun. **46**, 2977 (2010)
24. Qu, H., Shen, H., Li, J., Men, Y., Chen, X., Chong, Z.: Synthesis and characterization of three pentacene derivatives. Trans. Tianjin Univ. **24**, 453–460 (2018)
25. Pramanik, A., Sarkar, S., Pal, S., Sarkar, P.: Pentacene–fullerene bulk-heterojunction solar cell: a computational study. Phys. Lett. A **379**, 1036–1042 (2015)
26. Schweicher, G., Olivier, Y., Lemaur, V., Geerts, Y.H.: What currently limits charge carrier mobility in crystals of molecular semiconductors? Isr. J. Chem. **54**, 595–620 (2014)
27. Muz, I., Goktas, F., Kurban, M.: 3d-transition metals (Cu, Fe, Mn, Ni, V and Zn)-doped pentacene π-conjugated organic molecule for photovoltaic applications: DFT and TD-DFT calculations. Theor. Chem. Acc. **139**, 23 (2020)
28. Grimme, S., Ehrlich, S., Goerigk, L.: Effect of the damping function in dispersion corrected density functional theory. J. Comput. Chem. **32**, 1456–1465 (2011)
29. Becke, A.D.: A new mixing of hatree-fock and local density functional theories. J. Chem. Phys. **98**, 1372–1377 (1993)
30. Lee, C., Yang, W., Parr, R.G.: Development of the colle-salvetti correlation-energy formula into a functional of the electron density. Phys. Rev. B **37**, 785–789 (1988)
31. Frisch, M.J., Trucks, G.W., Schlegel, H.B., Scuseria, G.E., Robb, M.A., Cheeseman, J.R., Scalmani, G., Barone, V., Mennucci, B., Petersson, G.A., Nakatsuji, H., Caricato, M., Li, X., Hratchian, H.P., Izmaylov, A.F., Bloino, J., Zheng, G., Sonnenberg, J.L., Hada, M., Ehara, M., Toyota, K., Fukuda, R., Hasegawa, J., Ishida, M., Nakajima, T., Honda, Y., Kitao, O., Nakai, H., Vreven, T., Montgomery, J.A., Peralta, J.E., Ogliaro, F., Bearpark, M., Heyd, J.J., Brothers, E., Kudin, K.N., Staroverov, V.N., Kobayashi, R., Normand, J., Raghavachari, K., Rendell, A., Burant, J.C., Iyengar, S.S., Tomasi, J., Cossi, M., Rega, N., Millam, J.M., Klene, M., Knox, J.E., Cross, J.B., Bakken, V., Adamo, C., Jaramillo, J., Gomperts, R., Stratmann, R.E., Yazyev, O., Austin, A.J., Cammi, R., Pomelli, C., Ochterski, J.W., Martin, R.L., Morokuma, K., Zakrzewski, V.G., Voth, G.A., Salvador, P., Dannenberg, J.J., Dapprich, S., Daniels, A.D., Farkas, Foresman, J.B., Ortiz, J. V, Cioslowski, J., Fox, D.J.: Gaussian 09, Revision E.01 (2009)
32. Boys, S.F., Bernardi, F.: The calculation of small molecular interactions by the differences of separate total energies. Some procedures with reduced errors. Mol. Phys. **19**, 553–566 (1970)
33. Pearson, R.G.: The principle of maximum hardness. Acc. Chem. Res. **26**, 250–255 (1993)
34. Parr, R.G., Pearson, R.G.: Absolute hardness—companion parameter to absolute electronegativity. J. Am. Chem. Soc. **105**, 7512–7516 (1983)
35. O'Boyle, N.M., Tenderholt, A.L., Langner, K.M.: Cclib: a library for package-independent computational chemistry algorithms. J. Comput. Chem. **29**, 839–845 (2008)
36. Yanai, T., Tew, D.P., Handy, N.C.: A new hybrid exchange–correlation functional using the Coulomb-attenuating method (CAM-B3LYP). Chem. Phys. Lett. **393**, 51–57 (2004)
37. Muz, İ., Kurban, M.: Enhancement of electronic, photophysical and optical properties of 5,5′-Dibromo-2,2′-bithiophene molecule: new aspect to molecular design. Opto-Electron. Rev. **27**, 113–118 (2019)
38. Kurban, M., Gündüz, B., Göktaş, F.: Experimental and theoretical studies of the structural, electronic and optical properties of BCzVB organic material. Optik (Stuttg) **182**, 611–617 (2019)
39. Wong, B.M., Cordaro, J.G.: Coumarin dyes for dye-sensitized solar cells: a long-range-corrected density functional study. J. Chem. Phys. **129**, 214703 (2008)
40. Wong, B.M., Hsieh, T.H.: Optoelectronic and excitonic properties of oligoacenes: substantial improvements from range-separated time-dependent density functional theory. J. Chem. Theory Comput. **6**, 3704–3712 (2010)
41. Leong, K., Foster, M.E., Wong, B.M., Spoerke, E.D., Van Gough, D., Deaton, J.C., Allendorf, M.D.: Energy and charge transfer by donor–acceptor pairs confined in a metal-organic framework: a spectroscopic and computational investigation. J. Mater. Chem. A **2**, 3389–3398 (2014)
42. Foster, M.E., Azoulay, J.D., Wong, B.M., Allendorf, M.D.: Novel metal-organic framework linkers for light harvesting applications. Chem. Sci. **5**, 2081–2090 (2014)
43. Scharber, M.C., Mühlbacher, D., Koppe, M., Denk, P., Waldauf, C., Heeger, A.J., Brabec, C.J.: Design rules for donors in bulk-heterojunction solar cells—towards 10% energy-conversion efficiency. Adv. Mater. **18**, 789–794 (2006)
44. Campbell, R.B., Robertson, J.M., Trotter, J.: The crystal and molecular structure of pentacene. Acta Crystallogr. **14**, 705–711 (1961)
45. Dierksen, M., Grimme, S.: Density functional calculations of the vibronic structure of electronic absorption spectra. J. Chem. Phys. **120**, 3544–3554 (2004)
46. Kadantsev, E.S., Stott, M.J., Rubio, A.: Electronic structure and excitations in oligoacenes from ab initio calculations. J. Chem. Phys. **124**, 134901 (2006)
47. Maliakal, A., Raghavachari, K., Katz, H., Chandross, E., Siegrist, T.: Photochemical stability of pentacene and a substituted pentacene in solution and in thin films. Chem. Mater. **16**, 4980–4986 (2004)
48. Gruhn, N.E., da Silva, D.A., Bill, T.G., Malagoli, M., Coropceanu, V., Kahn, A., Bredas, J.L.: The vibrational reorganization energy in pentacene: molecular influences on charge transport. J. Am. Chem. Soc. **124**, 7918–7919 (2002)
49. Prasad, M.V.S., Sri, N.U., Veeraiah, V.: A combined experimental and theoretical studies on FT-IR, FT-Raman and UV–vis spectra of 2-chloro-3-quinolinecarboxaldehyde. Spectrochim. Acta Part A Mol. Biomol. Spectrosc. **148**, 163–174 (2015)
50. Parr, R.G., Yang, W.T.: Density functional-approach to the frontier-electron theory of chemical-reactivity. J. Am. Chem. Soc. **106**, 4049–4050 (1984)
51. Herve, P.J.L., Vandamme, L.K.J.: Empirical temperature-dependence of the refractive-index of semiconductors. J. Appl. Phys. **77**, 5476–5477 (1995)